PYRENE BASED SCHIFF BASES AS COLORIMETRIC AND RATIOMETRIC SENSORS

Thesis submitted in partial fulfilment of the requirements for the award of the

degree of

MASTER OF SCIENCE

IN

CHEMISTRY

Submitted By:

RAVNEET KAUR

Registration No. 301402017

Supervisor:

Dr. Vijay Luxami

School of Chemistry and Biochemistry

Thapar University

Patiala

July 2016

ACKNOWLEDGEMENTS

I would never have been able to finish my dissertation without the guidance of my supervisors, help from friends, and support from my family. I would like to express my deepest gratitude to my advisor, Dr. Vijay Luxami, for her tremendous guidance, patience, and providing me with an excellent atmosphere for doing research. She provided me with immense assistance in this project.

I would also like to thank Mr. Akul Sen Gupta for supervising my research for the past six months and helping me at each and every step in the entire process of my dissertation.

I am further grateful to Dr. Bonamali Pal and all the faculty members for their constant support. I would also like to acknowledge SAI Labs and Punjab University, Chandigarh for providing the NMR and Mass spectroscopy facilities respectively.

In the end, I want to thank my family and friends for always being so supportive of me and encouraging me with their love and best wishes.

CANDIDATE'S DECLARATION

This thesis titled "**Pyrene Based Schiff Bases as Colorimetric and Ratiometric Sensors**" is a presentation of my original research work. Wherever contributions of others are involved, every effort is made to indicate this clearly, with due reference to the literature, and acknowledgement of collaborative research and discussions. The work was done under the guidance of Dr. Vijay Luxami at Thapar University, Patiala.

Ravneet Kaur

RAVNEET KAUR

Patiala
Date: 8 July, 2016

In my capacity as supervisor of the candidate's thesis, I certify that the above statements are true to the best of my knowledge.

Vijay Luxami

Dr. Vijay Luxami

Supervisor

SCBC, Thapar University

Patiala

Dr. Bonamali Pal

Professor and Head

SCBC, Thapar University

Patiala

CERTIFICATE

This is to certify that the thesis "**Pyrene Based Schiff Bases as Colorimetric and Ratiometric Sensors**" is being submitted by Ravneet Kaur in partial fulfillment of requirements for the award of degree of Master's in Science in Chemistry in School of Chemistry and Biochemistry, Thapar University, Patiala, is a bonafide work carried out under the supervision of Dr. Vijay Luxami and the no part of the thesis has been submitted for the award of any degree.

Dr. Vijay Luxami
Assistant Professor and Supervisor,
School of Chemistry and Biochemistry,
Thapar University, Patiala

Dr. Bonamali Pal
Professor and Head
School of Chemistry and Biochemistry,
Thapar University,
Patiala, Punjab

Dr. S. S. Bhatia
Dean, Academic Affairs,
Thapar University,
Patiala, Punjab

Table of Contents

INTRODUCTION

Supramolecular chemistry is the domain of chemistry that is made up of discrete number of assembled molecular subunits. There are many forces which are responsible for spatial organisation vary from weak (intermolecular forces or hydrogen bonding) to strong (covalent bonding) provided that the degree of electronic coupling remains small between the molecular component and with respect to energy parameters of the component.[1] Supramolecular chemistry examines the molecule with weaker interactions while traditional chemistry based on the covalent bonding. Supramolecular chemistry includes molecular self – assembly, folding and recognition of molecules.[2-3]

Chemosensors are that which converts chemical signal into an action potential. Therefore it is also called as Chemoreceptor. It binds to a metal with a signalling unit such as chromophore or fluorophore. During interactions, metal ions cause a signal with binding units that result in change in absorption wavelength or emission intensity. Fluorescent chemosensors have high sensitivity that have been developed to be a useful tool to sense biological important species such as metal ions.[4] Fluorescent chemosensors contains a recognition site linked to a signal source which converts recognition event into the fluorescence signal.

Properties of ideal fluorescent chemosensors are:

1) The recognition site must have the strongest affinity for the relevant target.
2) It is also affected by the environmental interferences such as sensor molecular concentration and photobleaching.[5]

Signalling systems can be developed by using three main approaches:

1) "Binding site–signalling subunit": In this covalent bonds are present and electronic properties are changed by interaction of anions with binding sites.[6]
2) "Displacement"protocol: In this non covalent bonds are present and optical characteristics are changed by coordination of anion in the binding site. [7]
3) "Chemodosimeter" paradigm : In this fluorescence or colour are changed by anion induced reactions.[8]

In Supramolecular chemistry, recognition of anions and cations plays a very crucial role in chemical and biological applications. Anions and cations are of various types may vary from F^-, Cl^-, CN^-, Zn^{2+}, Cu^{2+}, Hg^{2+} etc. Due to the mild toxicity F^- plays a vital role in

the presence of food samples and in bone-growth.[9] By excess intake of F^- ion it causes skeletal fluorosis and nephrotoxic changes in humans.[10] CN^- has strong binding affinity due to this property it is very toxic to humans because in heme complexes it blocks the vacant sites of Fe^{3+} which inactivates the cellular respiration.[11] In catalytic centres, Zn^{2+} is considered as important cation because of its many properties in biological process such as gene transcription, reproduction of mammalian.[12] The electronic configuration of Zn^{2+} is d^{10} due to this Zn^{2+} is tightly bound with proteins and free Zn is present in tissues such as brain and pancreas. By excess use of Cu ions cause lethargy, increased blood pressure and vomiting.[13] Due to their severe effects on microorganisms it can disrupt the natural ecosystems. By excess use of Cd^{2+} can cause prostrate lung, breast, or endometrial cancer.[14] Fluorescence sensing of anions and cations can be detected by different processes. There are four processes are as under:

1) Internal charge transfer (ICT).
1) Photo-induced electron transfer (PET).
2) Metal-ligand charge transfer (MLCT).
3) Excited state intramolecular proton transfer (ESIPT).[15]

Excited state intramolecular proton transfer has great advantage out of these above processes because of their vast applications in supramolecular chemistry. It also has significant influence on optical responses, such as UV/Vis and fluorescence spectroscopy. Fluorescence spectroscopy is time resolved spectroscopy and provides information about photophysical properties.[16] As compared to normal fluorophores, ESIPT provides the large stokes shift due to this inner-filter effect or self absorption can be avoided. The ESIPT process requires a proton donor (–OH, $–NH_2$) and a proton acceptor (–C=O, –N) groups in close proximity to form the intramolecular hydrogen bond. The mechanism provides three steps: First, there should be an intramolecular hydrogen bond (X–H···Y) in the sensor molecule, and the molecule could undergo an ESIPT process from the hydrogen-bond donor (X–H) to hydrogen-bond acceptor (Y). Then, the introduced anion (A) could form a hydrogen bond X–H···A with X–H instead of the acceptor Y and inhibit the ESIPT process. ESIPT chromophores is the transient nature of the ground state of the emissive species of the ESIPT chromophores, i.e. the keto tautomer. From the original excited form photochemical process produces a tautomer with a different electronic structure. It is a four-level photo-cycle (E - E* - K* - K) scheme implemented by the enol (E) - keto (K) photo tautomerisation process.[17]

ESIPT process rate depends on donor/acceptor groups. Attractive properties of ESIPT chromophores are dual emissions, short wavelength emission due to the excited state enol form (E*) (normal emission) and the longer one due to the excited state keto form (K*) (ESIPT emission) through a four-level photocycle. This process generates different transient species due to this ESIPT emission gets highly affected by its microenvironment that results in changing in properties of fluorescence.

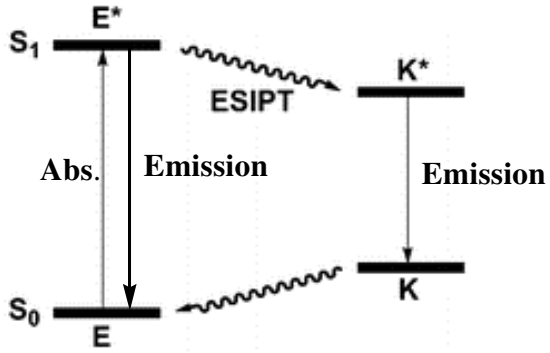

There are number of Schiff base colorimetric sensors had been used, Schiff bases were capable of forming coordinate bonds with many of metal ions through phenolic group and azomethine groups.[18] Schiff bases were recognize the metals through these binding sites, because of this reason these were used to construct a sensor as a sensing materials.[19] A large number of Schiff bases and their complexes attract significant interest and attention because of their biological activity including antibacterial and fungicidal properties and catalytic activity.[20]

Review of Literature

Santillan *et al.* synthesized two Schiff bases **1** and **2** which exhibited selectivity and fluorescence turn "on-off" effect upon zinc binding in water : methanol (95 : 5, v/v, 10 mM HEPES). In the case of compound **1**.Zn^{2+}, on the addition of $Cu^{2+,}$ emission process was quenched which results in compound **1**·Cu^{2+} complex "*off-on*" displacement approach.[21] However, Cu^{2+} had no interference with the zinc ions in the case of compound **2**·Zn^{2+} which was a typical problem for Zn^{2+} sensors. During transition, structural change in the ligand from the enol-imine tautomer in compound **1** to the keto-enamine tautomer in compound **2** was enough to modulate the Zn^{2+}/Cu^{2+} selectivity. Moreover, we found that the interaction between both **1**·Zn^{2+} and **2**.Zn^{2+} complexes and tartrate anions completely restored the free ligands by the tartrate substitution mechanism..

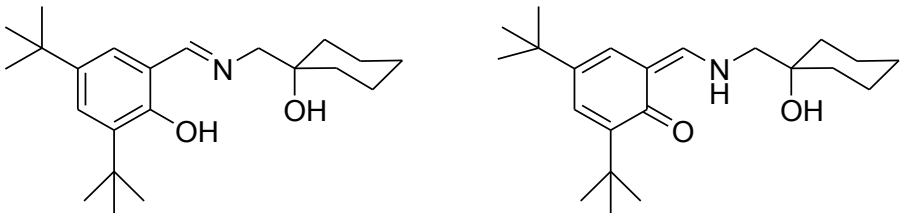

1 **2**

Zhou *et al.* Designed Fe(III) complex with 1, 8-naphthalene-based Schiff base unit **3** and **4** which showed turn-on fluorescent sensors for PO_4^{3-}. In both solution and solid-state film, phosphate anions such as HPO_4^{2-}, H_2PO_4 exhibited high selectivity and sensitivity.[22]

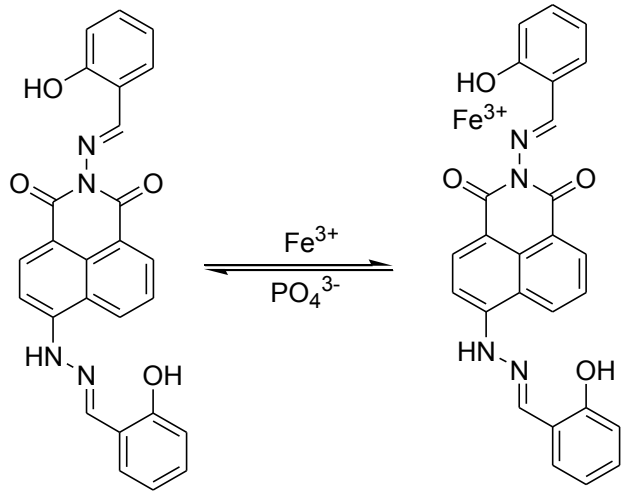

3 **4**

Mobin *et al.* synthesized imine conjugate Schiff base ligand **5** and showed selectivity towards Zn^{2+}. UV-vis, fluorescence and ^1H NMR techniques were used to detect the sensing behaviour of compound. With a detection limit of 1.47 μM, Compound **5** showed fluorescence switch "*ON*" with the Zn^{2+} ion. Binuclear complex was formed upon binding the Zn^{2+} ions and confirmed by single crystal X-ray studies.[23] Furthermore; both compounds were found to had marginal toxicity against MCF-7 and A375 cell lines.

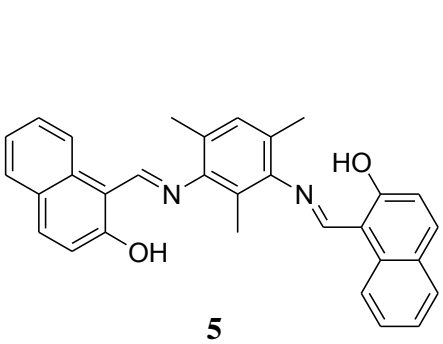

5

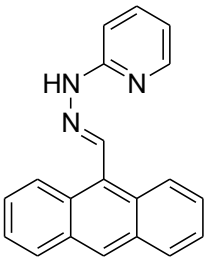

6

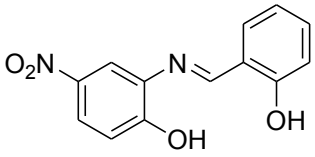

7

Fu-Hsiang and their co-workers synthesized a Schiff base compound **6** which showed fluorescent ''off–on'' detection of Cu^{2+} ions, via PET-based mechanism.[24] The PL titrations of **6**.Cu^{2+} complex was calculated from Job's plot and the binding sites were supported by ^1H NMR titration. By standard deviation, the detection limit (LOD) and association constant (K_a) of complex **6**.Cu^{2+} were obtained. By confocal fluorescence microscopy imaging, the analysis of Cu^{2+} ions in living cells compound **6** was used as effective fluorescent probe.

M. Hijji *et al.* was developed a Schiff base **7** which was a colorimetric anion sensor. The bathochromic shift from 342 to 450 nm and color changed was obtained upon addition of fluoride, acetate and dihydrogen phosphate (DHP) ions and due to another anions such as chloride, hydrogen sulphate, no color changed was observed.[25] The binding order of $AcO^- \approx F^- >> H_2PO_4^-$ showed by binding constants and the formation of a (1:1) complex (receptor : anion) with fluoride, acetate was indicated by Job's plot. In the solid state, the Schiff base indicated that keto-amine tautomer was existed in the compound.

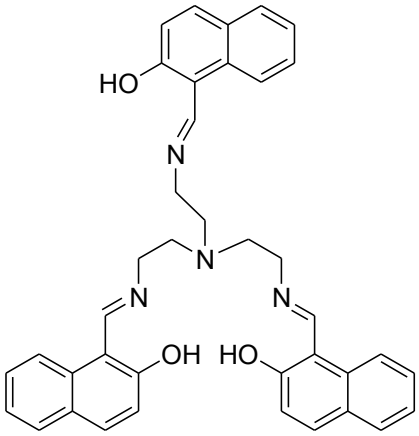

8

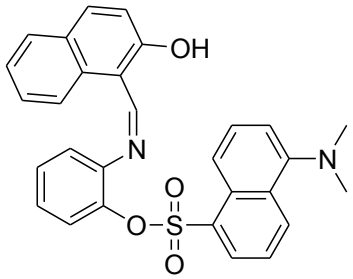

9

Wu *et.al* was prepared fluorescent Schiff base receptor **8** which exhibited high selectivity towards Zn^{2+} ion on '*OFF-ON-TYPE*' mode.[26] The selectivity for Zn^{2+} was the consequence of combined effects of chelation-enhanced fluorescence (CHEF), C=N isomerization, and inhibited of photoinduced electron transfer (PET).

Metal ions and anions sensing properties of bi-functional Schiff base fluorescent sensor **9** was investigated and prepared by Wu et.al which exhibited selective fluorescence response towards Al^{3+} and colorimetric response (yellow to colorless) towards CN^- ion.[27] The detection limits 14 nM and 73 nM, were determined to Al^{3+} and CN^- of receptor which was low to detect nano-molar concentration of Al^{3+} and CN^-.

Velmathi *et al.* synthesized Schiff bases receptors **10** and **11** which showed high sensitivity towards Fe^{3+}, Cu^{2+}, Hg^{2+} and Cr^{3+} in aqueous medium.[28] Colorimetric and optical - emission spectroscopic studies were used to detect the sensing ability of receptors and Job's plot was used to determine 2:1 binding stoichiometries of receptor. The colorimetric receptors with low detection limit of μM levels exhibited high sensitivity. Due to the photo induced electron transfer mechanism both the receptors showed fluorescence quenching in the presence of metal ions. By using Stern–Volmer plot, quenching constant was determined.

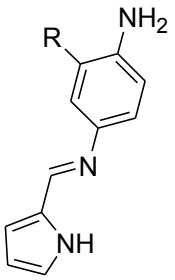

10 R = H

11 R = -NO_2

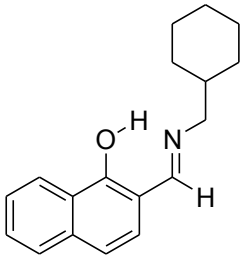

12

Guhhait and Co-workers synthesized and characterized a Schiff base compound **12** by spectroscopic techniques (^{1}HNMR and FT-IR). With photo-induced electron transfer (PET), low emission yield of the compound from the imine receptor moiety to the naphthalene fluorophore unit has been rationalized in anticipation.[29] The promising prospect of the compound **12** as a chemosensor for Cu^{2+} and Zn^{2+} ions through remarkable fluorescence enhancement had been revealed by the transition metal ion-induced modification of the fluorophore-receptor communication. By strong binding interaction, selectivity for these two metal ions had been interpreted on the grounds. Efficient synthetic procedure and chemosensory activity of the compound had been used to detect the aforesaid transition metal ions to the level of micro-molar concentration (detection limit being 2.74 and 2.27 ppm respectively).

Shen *et al.* synthesized two new Schiff base derivatives **13** and **14** which was characterised by spectroscopy techniques (^{1}H NMR and FT-IR). By X-ray single crystal structure of compound **14** had been determined.[30] Both the compounds were poorly fluorescent and displayed sensitive fluorescence responses to a panel of 24 mono-valent, divalent, and trivalent metal ions in CH_3CN–DMSO (9:1, v/v) had been revealed by the analysis of fluorescence properties of the compounds. Imine **13** showed red shifts in emission and increase in intensity with Fe^{3+}, Cu^{2+}, Zn^{2+}, Cd^{2+}, Mn^{2+}, Zr^{4+}, Hg^{2+}, Cr^{2+}, Pb^{2+}, Sn^{2+}, Bi^{2+}, Al^{3+}, Ce^{3+}, La^{3+}, Sm^{3+}, Gd^{3+}, Nd^{3+}, Eu^{3+} and Dy^{3+}. The compound **14** showed enhancements in emission intensity coupled with red shifts towards Zr^{4+}, Sn^{2+}, Al^{3+} and Zn^{2+} and strong quenching towards Fe^{3+}. The fluorescence enhancement mechanism of **13** and **14** for metal ions was assumed to be based on C=N isomerisation.

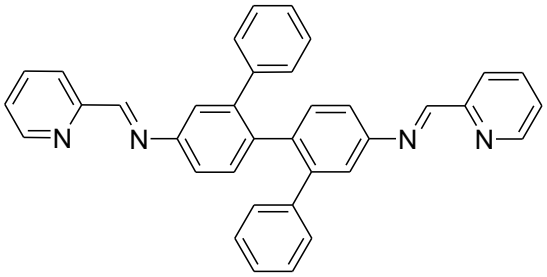

13

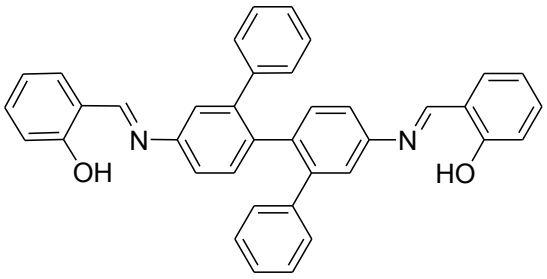

14

A Schiff base **15** has been synthesized as an anion receptor by Guchhait *et al.*[31] Which showed high selectivity towards F^- and AcO^- ions due to the presence of conjugated imine, phenolic –OH and electron withdrawing substituent nitro ($–NO_2$). By UV–vis spectral changes, recognition properties had been investigated though naked-eye color change (colorless to yellow). Density functional theory (DFT) was used to predict the stoichiometeries of the complexes between receptor and anions.

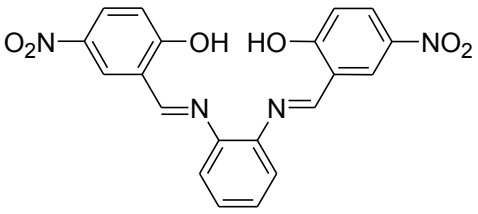

15

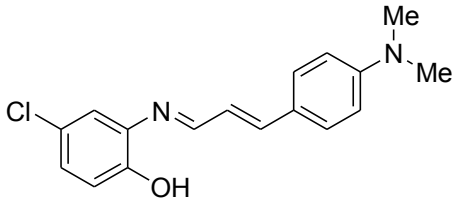

16

Ramos-Ortiz *et al.* synthesized a schiff base derivative **16** which showed sensitive colorimetric response towards Ni^{2+} in aqueous solution.[32] The compound showed large red shift in the absorption peak from 435 to 480 nm and color changed from faded yellow to deep orange by addition of nickel in water. By absorption spectroscopy, detection limit was measured for Ni^{2+} in water of 1×10^{-7} M whereas by naked eye the detection limit was of the order of 5×10^{-6} M. The compound **16** showed the minimal spectral changes upon interaction with other metal ions such as Hg^{2+}, Pb^{2+}, Co^{2+}, Cu^{2+} and Mn^{2+}. These results showed that the detection in water over a pH range of 5.5–8 was measured by Schiff base **16**.

Yang *et al.* designed and synthesized a chromone schiff-base receptor **17** and displayed fluorescence enhancement and fluorescence turn "*OFF–ON*" for Al^{3+} ion in ethanol solution.[33] The probe showed visible light excitation (423 nm) and emission (507 nm) color

changed from colorless to yellow-green upon binding of Al^{3+}. No such effect on the fluorescence was investigated by other metal ions. The detection limit of the sensor **17** towards Al^{3+} was low as $5x10^{-8}$ M, which was satisfactory for monitoring Al^{3+} levels in physiological and environmental systems.

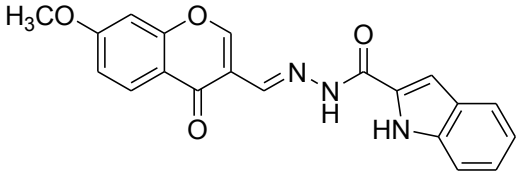

17

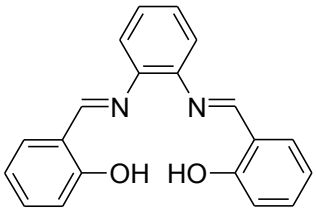

18

Velmathi *et al.* designed a schiff base chromogenic receptor **18** which showed high selective binding with Zn^{2+} ion.[34] Receptor **18** showed colorimetric response towards Zn^{2+} ions in aqueous medium and fluorescent response by sensing other metal ions like Pb^{2+}, Hg^{2+}, Sn^{2+} and Cd^{2+}. Due to the inhibition of the (ESIPT) mechanism, receptor exhibited fluorescence enhancement upon binding with Zn^{2+} ion.

Gupta *et al.* synthesized a schiff base **19** and **20** as metal ion receptors and showed colorimetric response from colorless to yellowish-brown for Cu^{2+} ions and colourless to yellow for Co^{2+}, Ni^{2+}, Cd^{2+} and Zn^{2+} in methanol solution.[35] The detection limit was allowable to 1.0×10^{-5} and 1.0×10^{-6} M level of Cu^{2+}, 1.0×10^{-4} and1.0×10^{-5} M level of Co^{2+}, Ni^{2+}, Cd^{2+}, Zn^{2+} according to visual colour change and UV–Vis spectral change.

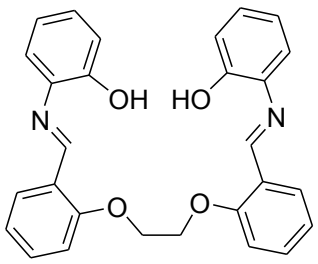

19

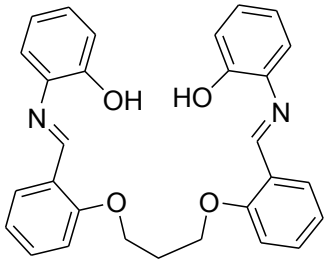

20

Yen *et al.* synthesized a receptor **21** which showed high selectivity towards Cu^{2+} and Fe^{3+} by UV-Vis and fluorescent color changes in aqueous solution ($DMSO/H_2O$ = 8/2, v/v).[36] The sensitivity towards Cu^{2+} or Fe^{3+} was not interfered by the presence of other metal ions such as Mg^{2+}, Cd^{2+}, Ag^{+}, Zn^{2+}, Ni^{2+}, Co^{2+}, Mn^{2+}, Cr^{3+}, Ca^{2+}, Na^{+}, Pb^{2+}, K^{+}, Fe^{2+}, Li^{+} and Hg^{2+} ions.

The receptor was used for the detection of Fe^{3+} ion, which developed a good image of the biological organelles.

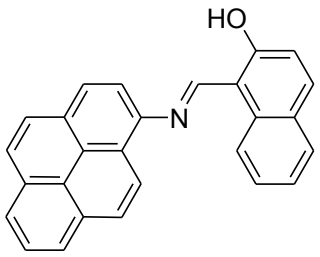

21

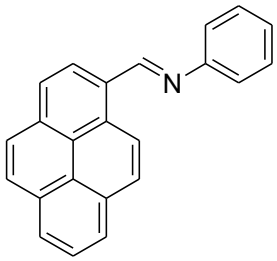

22

Chellappa *et al*. synthesized, and evaluated a new pyrene-based ‘‘*turn on”* fluorescent chemosensor **22** which showed remarkable enhanced fluorescence intensity in the presence of Hg^{2+} ions and a high selectivity towards Hg^{2+} ions over a wide range of metal ions in aqueous acetonitrile.[37] The probe showed selectivity and sensitivity with a 12-fold enhancement in fluorescence towards Hg^{2+}. Upon the addition of Hg^{2+} ions, the probe displayed an apparent color change, which could be observed by the naked eye under a UV lamp. The *in vitro* sensitivity to Hg^{2+} was demonstrated in candida albicans cells with the use of confocal microscopy.

Shellaiah and their co-workers synthesized schiff base derivative **23** via a one-pot reaction and utilized as a fluorescence turn-on probe for Hg^{2+} ion detection along with live cell imaging. Compound **23** in DMSO/H_2O (v/v = 7/3; pH 7.0) showed fluorescence turn-on response to Hg^{2+} ions, *via* chelation enhanced fluorescence.[38] The 2 : 1 stoichiometry of the sensor complex **23**.Hg^{2+} was calculated from the Job`s plot based on UV-Vis absorption titrations. In addition, the binding sites of the sensor complex **23**.Hg^{2+} were well established from the ^{1}H NMR titrations and ESI-mass analysis. The fluorescence reversibility of **23**.Hg^{2+} complex was revealed via the consequent addition EDTA. Moreover, pH effect and density functional theory studies were investigated for the **23**.Hg^{2+} sensor system. Confocal fluorescence microscopy imaging in Hela cells showed that **23** could be used as an effective fluorescent probe for detecting Hg^{2+} in living cells.

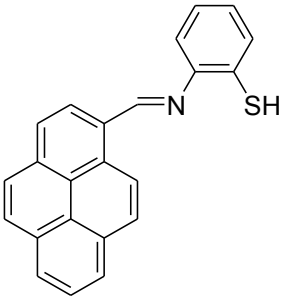

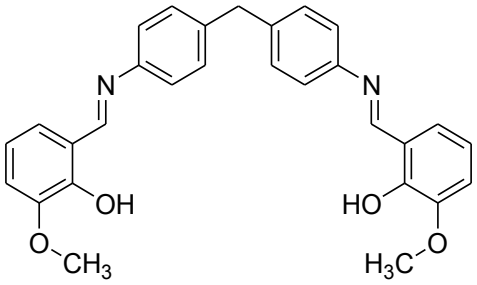

23 **24**

Bi *et al.* synthesized a schiff base compound **24** and characterized by elemental analysis, ^{1}H NMR, ^{13}C NMR, IR, electronic absorption spectra and X-ray diffraction single crystal analysis.[39] The compound **24** did not show any fluorescence intensity in a range of 450–650 nm, but its fluorescence spectrum shows enhancement in the intensity of the signal at 372 nm on binding with the Zn(II) cation from pH 6 to 14. No such significant change was observed for other metal ions. Fluorescence intensity was linear with concentration of Zn (II) cation in a range from 1×10^{-7} mol·L^{-1} to 1.2×10^{-5} mol·L^{-1}.

Yang *et al.* synthesized Schiff-base chemosensor **25** for Cu^{2+} and fluorescence quenching only for Cu^{2+} demonstrates that ligand **25** exhibits high selectivity and efficient signaling behaviour toward micromolar concentration of Cu^{2+} compared with other metal ions.[40] The coordination form between ligand and Cu^{2+} was elucidated *via* crystal structure.

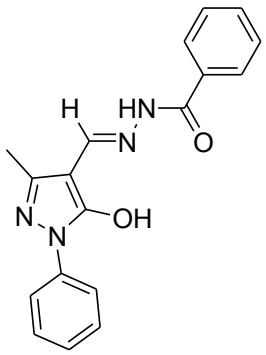

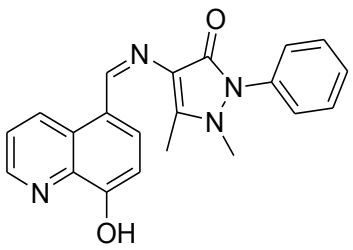

25 **26**

Yang *et al.* synthesized a fluorescent sensor **26** based on 8-hydroxyquinoline and antipyrine. This fluorescent sensor exhibited high selectivity for Al^{3+} over other metal ions with the detection limit reaching below 10^{-7} M under weak acid aqueous conditions. Wu et al. synthesized a simple schiff-base receptor **27**. It exhibited an "OFF-ON" type mechanism with high sensitivity in the presence of Al^{3+}. The receptor **27** exhibited a high association constant with sub-micromolar detection for Al^{3+} in EtOH–H_2O (95:5 v/v) solution.[42] The addition of

EDTA quenches the fluorescence of the receptor **27**: Al^{3+}complex offering receptor **27** as a reversible chemosensor.

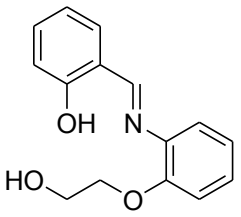

27

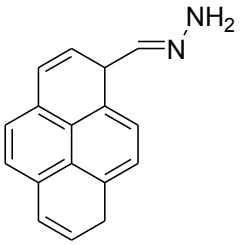

28

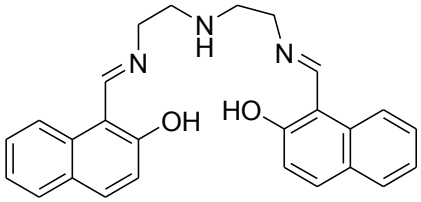

29

Panja and their co-workers synthesized a pyrene-based simple fluorosensor **28**. It exhibited high selectivity towards Cu^{2+} ions via fluorescence enhancement of monomer and excimer emission.[43] The origin of excimer formation was examined and established to be of static in nature from the study of absorption and excitation spectra. The observed monomer and excimer emission in the presence and absence of Cu^{2+} ion with varying pH was studied. The effect of varying portions of water content in solvent on the sensor molecule was also examined. The sensor found trace amount of Cu^{2+} ions present in drinking water samples from various sources. The detection limit of the **28** sensor was found to be 4×10^{-8} M.

Mukherjee *et al.* synthesized an efficient fluorescent Al^{3+} receptor **29** by the condensation reaction between 2-hydroxy naphthaldehyde and diethylenetriamine. High selectivity and affinity of compound **29** towards Al^{3+} in ethanol and HEPES buffer at pH 7.4, makes it suitable to detect intracellular Al^{3+} with fluorescence microscopy.[44] The lowest detection limit for Al^{3+} was 3.0 X 10^{-7} M and 1.0 X 10^{-7} M in EtOH and HEPES buffer respectively.

Objective

From the literature survey, we have found that Schiff bases were used for sensing purposes through different techniques such as PET, ESIPT etc. In addition Schiff bases also respond as colorimetric sensors. Moreover, the chelating ability of schiff bases make them important in sensing to different ions through coordinates bonds. There are only the few reports where schiff`s bases have been used as fluorescent sensors. Based on these following objectives were proposed:

1. Synthesis of pyrene based schiff bases with varied aromatic character.
2. Photophysical studies of pyrene based schiff bases.
3. Sensing ability of compounds towards various metals and anions.

Results & Discussions

Schiff bases have been used as colorimetric sensors are especially attractive, as it may allow "naked-eye" detection of the analyte without using any expensive equipment. Also Schiff bases are capable of forming coordinate bonds with many of metal ions through phenolic group and azomethine groups. Thus, in the present research project we emphasised on synthesis of Schiff bases based on pyrene moiety.

Synthesis of compound 1: Salicyladehyde (0.5 g, 4.09 mmol) and Hydrazine hydrate (1.99 ml, 24.09 mmol) were dissolved in 20 ml dry ethanol. The reaction mixture was cooled to 4 ^{o}C and after 5 min of stirring, precipitates was formed. The solid was filtered and washed with cold ethanol, to get the compound **1** as white solid (335 mg, 85% yield).

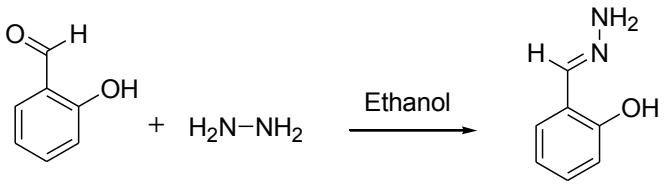

1

Synthesis of compound 1

Synthesis of Probe 3 – The solution of **1** (0.1 g, 0.73 mmol) and 1-pyrenecarboxaldehyde (0.16 g, 0.69 mmol) in 10 ml dry methanol was refluxed overnight. The completion of reaction was monitored through TLC, the reaction mixture was allowed to cool to room temperature. The separated solid was filtered and washed with cold methanol to get the pure probe **3** as yellow colored solid (85 mg, 90% yield, m.p. 240-241^{0}C) (**Scheme 1**).

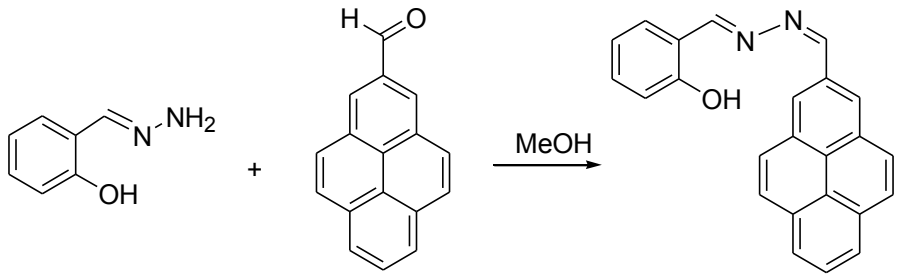

1 **2** **3**

Scheme 1: Synthesis of probe 3

^{1}H NMR ($CDCl_3$ + DMSO-d_6, 400 MHz) showed 1H broad singlet at δ 11.47 for OH, 1H singlet at δ 9.88 for HC=N, 2H multiplet at δ 9.16-9.13 for HC=N and aromatic-H, 1H

doublet at δ 8.74-8.72 for aromatic-H, 6H multiplet at δ 8.43-8.25 for aromatic-H, IH multiplet at δ 8.17-8.13 for aromatic-H, 1H doublet at δ 7.74 for aromatic-H, 1H triplet at δ 7.42 for aromatic-H, 2H multiplet at δ 7.02-7.00 for aromatic-H; ^{13}C NMR ($CDCl_3$ + DMSO-d_6, 100 MHz): δ 164.4, 161.7, 159.2, 133.2, 132.8, 132.1, 132.0, 130.8, 130.3, 130.1, 129.2, 129.0, 127.2, 126.5, 126.4, 126.2, 126.0, 125.0, 124.3, 123.8, 123.0, 119.4, 118.0, 116.6 (ArH) and mass spectra showed m/z peak at 363.12, confirming the structure for probe **3.**

Synthesis of compound 4: 2-Hydroxy-1-napthaldehyde (0.5 g, 2.90 mmol) and hydrazine hydrate (2.82 ml) were dissolved in 20 ml dry ethanol. The reaction mixture was cooled to 4 ^{o}C and after 5 min of stirring, precipitates was formed. The solid was filtered and washed with cold ethanol, to get the compound **4** as white solid (313 mg, 75% yield).

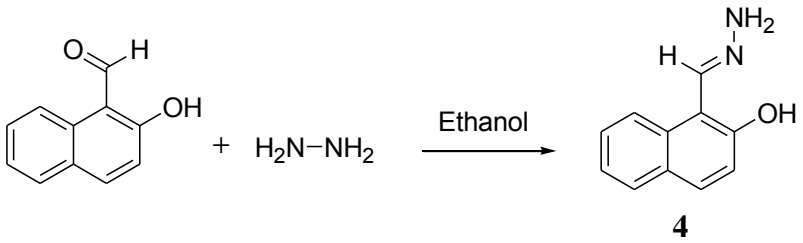

4

Synthesis of compound 4

Synthesis of Probe 5: The solution of **4** (0.1 g, 0.53 mmol) and 1-pyrenecarboxaldehyde (0.12 g, 0.52 mmol) in 10 ml dry methanol was refluxed overnight. After completion of the reaction, reaction mixture was allowed to cool to room temperature. The mixture was filtered and washed with cold methanol, to get the pure probe **5** as yellow colored solid (85 mg, 90 % yield, m.p 247-248^{0}C) (**Scheme 2**).

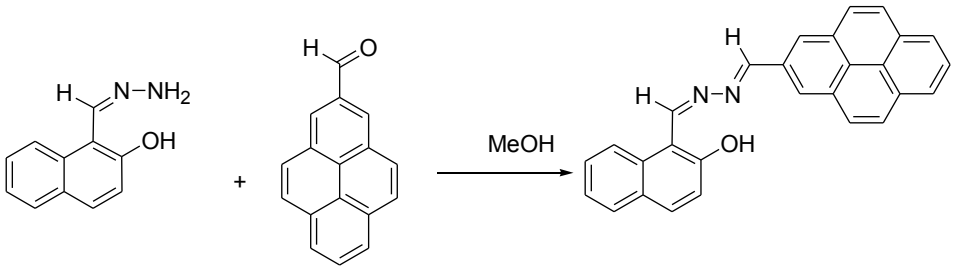

4 **2** **5**

Scheme 2: Synthesis of probe 5

^{1}H NMR ($CDCl_3$ + DMSO-d_6, 400 MHz) showed 2H quartet at δ 9.92 for two HC=N, four 1H doublets at δ 9.14, δ 8.76, δ 8.53 and δ 8.46 for aromatic-H, 5H multiplet in the range of δ 8.40-8.17 for aromatic-H, three 1H triplet at δ 8.09, δ 7.95 and δ 7.85 for aromatic-H, 1H quartet in the range of δ 7.66-7.54 for aromatic-H, 1H quartet in the range of δ 7.41-7.36 for

aromatic-H, 1H triplet at δ 7.23 for aromatic-H; ^{13}C NMR ($CDCl_3$ + DMSO-d_6, 100 MHz): δ 161.5, 161.0, 160.6, 160.2, 134.5, 133.2, 131.0, 130.7, 130.2, 129.2, 129.0, 128.8, 127.9, 127.3, 126.6, 126.2, 125.0, 123.7, 123.5, 121.3, 120.7, 118.9, 118.7, 108.5, 108.2 (ArH), confirming the structure for probe **5.**

Photo-physical properties of Probes 3 and 5

Probe **3** (20 µM, CH_3CN) showed an absorption band at 390 nm and 415 nm and emission band at 580 nm after exciting at 390 nm whereas probe **5** displayed an absorption band at 415 nm and emission band at 525 nm after exciting at 420 nm (Figure 1).

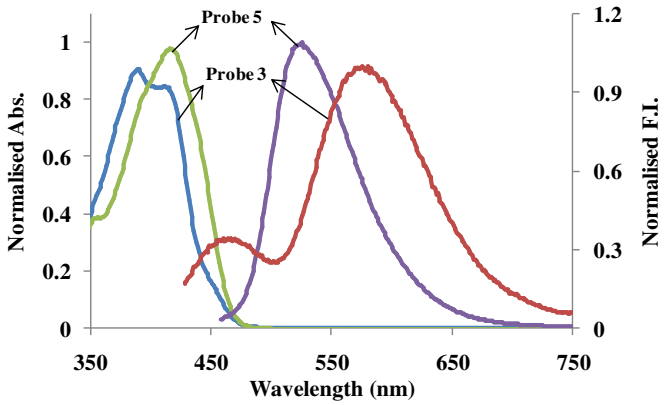

Figure 1: Normalized graph of absorption and emission spectrum of probe **3** and **5**.

Effect of various anions on absorption spectrum of Probe 3 and 5

The chromogenic sensing ability of probe **3** and **5** were studied in CH_3CN in the presence of 1000 µM of different anions (CN^-, F^-, Cl^-, Br^-, AcO^-, I^-, HSO_4^-, NO_3^-, SCN^-, $H_2PO_4^-$). In case of probe **3**, absorption changes was observed in the presence of F^- ion and in case of probe **5** color changes in the presence of F^- and CN^- ions was observed (Figure 2 and 3).

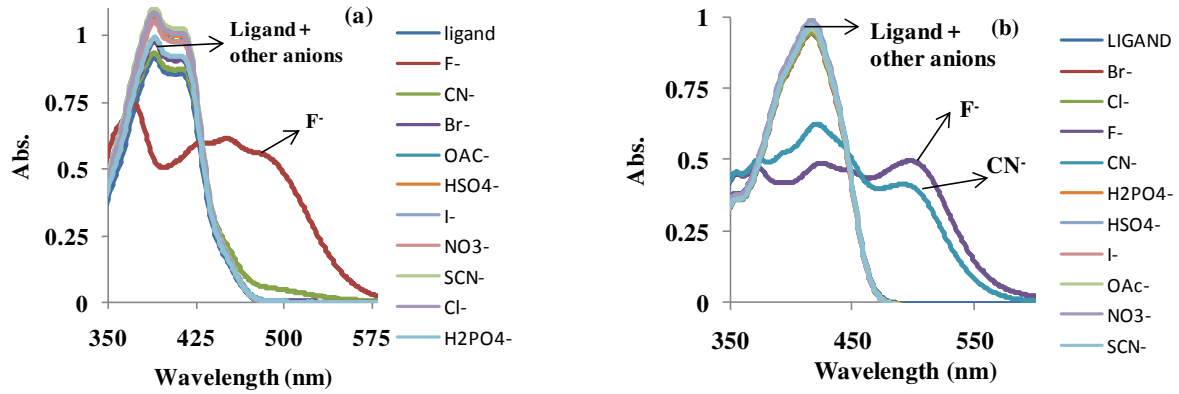

Figure 2: (a) Effect of various anions on absorption spectra of probe **3** (20 µM, CH_3CN); (b) Effect of various anions on absorption spectra of probe **5** (20 µM, CH_3CN).

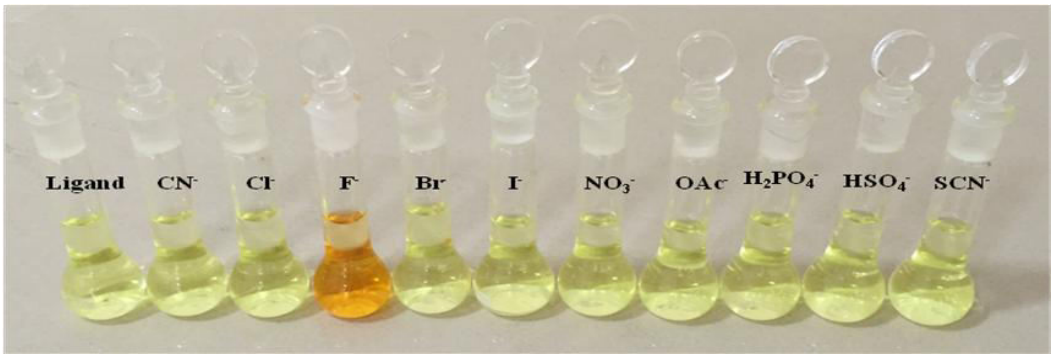

Figure **3**: (a) Photographs of probe **3** in the presence of different anions at 20 µM in CH_3CN.

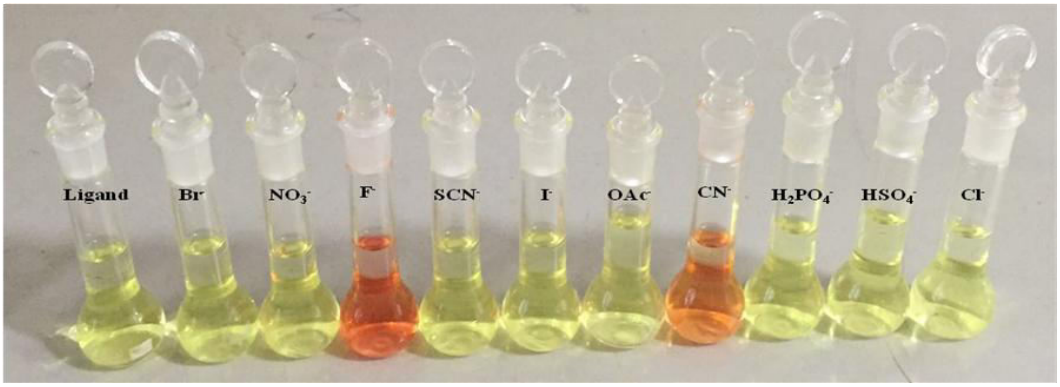

Figure **3**: (b) Photographs of probe **5** in the presence of different anions at 20 µM in CH_3CN.

Upon addition of F^- ions two new bands were observed at 455 and 490 nm indicating red shift of 75 nm. Upon gradual addition of F^- ions to the solution of Probe **3** (20 µM, CH_3CN), absorption bands at 390 nm and 415 nm diminished steadily with simultaneous formation of new bands at 455 and 490 nm with a clear isobestic point at 430 nm till addition of 1000 µM of F^- ion (Figure 4a), with detection limit of 50 µM. The Fluoride addition resulted in decrease in absorption intensity at 415 nm and increase at 490 nm provided an opportunity to determine fluoride ion ratio metrically. The absorption ratio at 490 and 415 nm varied from 0.0011 to 0.9655 indicating 825.21 fold absorption ratio changes (Figure 4b). Thus, probe **3** can be used to estimate an extensive range of fluoride ion between 50-1000 µM through ratio metric approach.

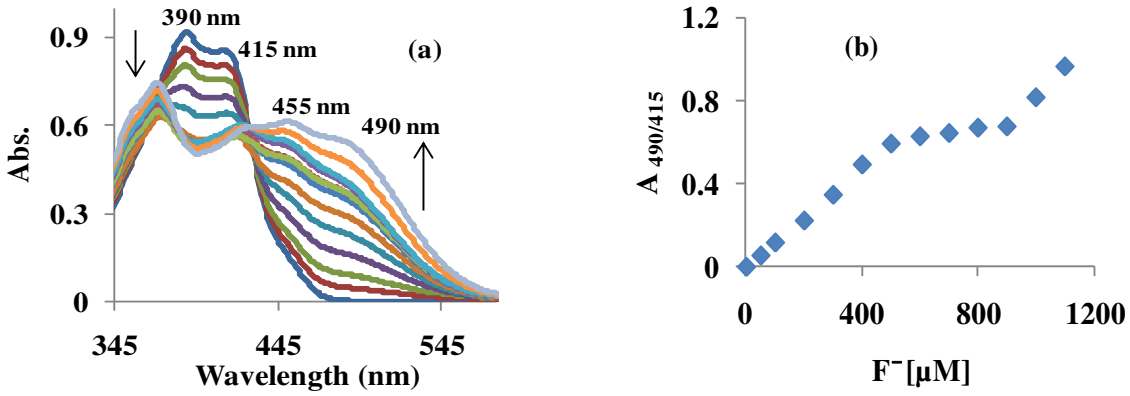

Figure 4: (a) Effect of incremental addition of fluoride ion on absorption spectrum of probe **3** (20 µM, CH_3CN); (b) Ratio-metric response between 490 and 415 nm (A_{490} / A_{415}) vs [F^-] ions on incremental addition of fluoride ions to probe **3** (20 µM, CH_3CN).

Upon addition of F^- ion to probe **5** formation of new band at 500 nm indicating red shift of 85 nm. Upon gradual addition of F^- ions to the solution of Probe **5** (20 µM in CH_3CN), absorption band at 415 nm diminished steadily with simultaneous formation of new band at 500 nm with a clear isobestic point at 450 nm till additions up to 508 µM of F^- ions, with detection limit of 1 µM (Figure 5a). The Fluoride addition resulted in decrease in absorption intensity at 415 nm and increase at 500 nm provided an opportunity to determine fluoride ion ratio metrically. The absorption ratio varied from 0.0022 to 1.061 at 415 and 500 nm indicating 482.27 fold absorption ratio change (Figure 5b). Thus, probe **5** can be used to estimate an extensive range of fluoride ion between 1-508 µM through ratio metric approach.

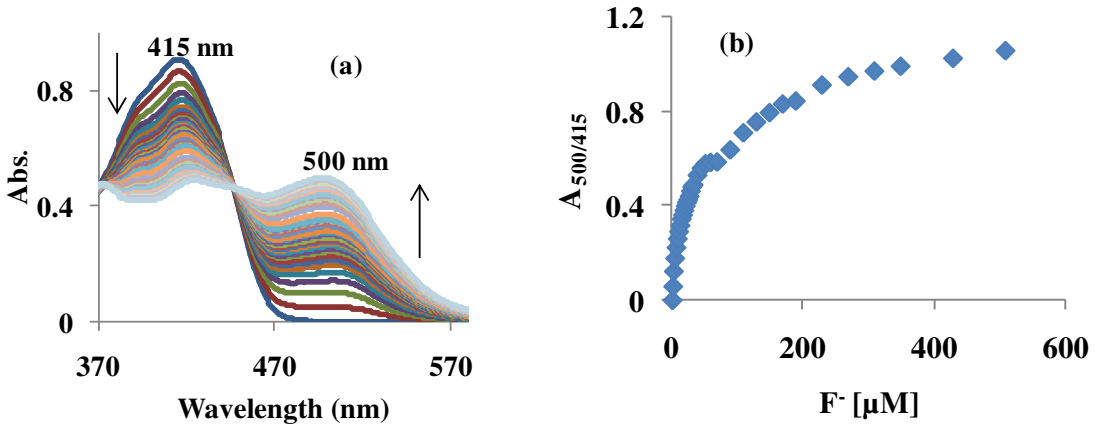

Figure 5: (a) Effect of incremental addition of fluoride ion on absorption spectrum of probe **5** (20 µM, CH_3CN); (b) Ratio-metric response between 415 and 500 nm (A_{500} / A_{415}) vs [F^-] ions on incremental addition of fluoride ions to probe **5** (20 µM, CH_3CN).

On the other hand, upon addition of CN^- ion to probe **5** formation of new band in the absorption spectra by 515 nm indicating red shift of 100 nm. Upon gradual addition of CN^- ion to the solution of Probe **5** (20 µM in CH_3CN), absorption band at 415 nm diminished steadily with simultaneous formation of new band at 515 nm with a clear isobestic point at 445 nm till additions up to 1576 µM of CN^- ions, with detection limit of 2 µM (Figure 6a). The cyanide addition resulted in decrease in absorption intensity at 415 nm and increase at 515 nm provided an opportunity to determine cyanide ion ratio metrically. The absorption ratio varied from 0.00103 to 0.5326 at 415 and 515 nm indicating 517.08 fold absorption ratio changes (Figure 6b). Thus, probe **5** can be used to estimate an extensive range of cyanide ions between 2-1576 µM through ratiometric approach.

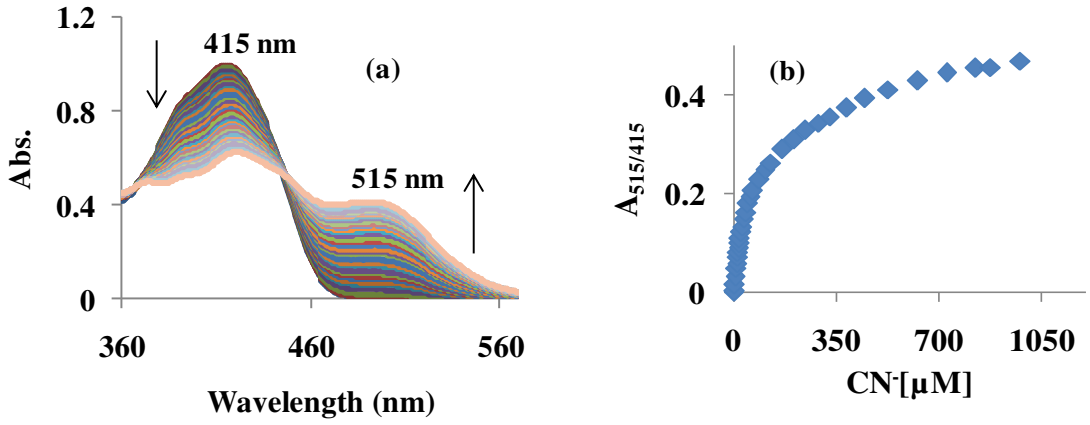

Figure 6: (a) Effect of incremental addition of cyanide ion on absorption spectrum of probe **5** (20 µM, CH_3CN); (b) Ratio-metric response between 415 and 515 nm (A_{515} / A_{415}) vs [CN^-] ions on incremental addition of cyanide ions to probe **5** (20 µM, CH_3CN).

Effect of various anions on emission spectrum of Probe 3 and 5

The probe **3** (20 µM, CH_3CN) on excitation at 390 nm exhibited emission band at 470nm and 580 nm. On addition of various anions, no significant change was observed except for F^- ion in case of probe **3** (Figure 7a). The fluorescence quenching was observed in case of F^- ions. To check the binding behaviour of probe **3** towards F^- ion, solution of probe **3** was titrated against F^- ion. We established that upon addition of 600 µM of F^- ion, fluorescence intensity was completely quenched (Figure 7b). Consequently, probe **3** can be used to estimate a wide range of flouride ions between 50-600 µM.

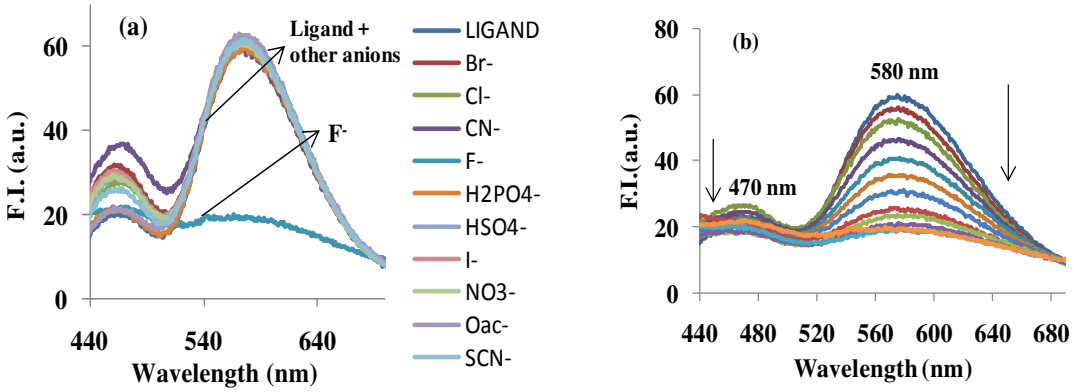

Figure 7: (a) Effect of various anions on emission spectra of probe **3** (20 μM, CH_3CN); (b) Effect of addition of F^- ions on emission spectrum of probe **3** at 20 μM in CH_3CN.

The probe **5** (20 μM, CH_3CN) on excitation at 420 nm exhibited emission band at 525 nm. On addition of various anions, no significant change was observed except for F^- and CN^- ions (Figure 8a). The fluorescence quenching was observed in case of CN^- and F^-. To check the binding behaviour of probe **5** towards F^- ions, solution of probe **5** was titrated against F^- ions. It was established that upon addition of 644μM of F^- ions, fluorescence intensity was completely quenched (Figure 8b). The binding constant was calculated to be 5.31 X 10^4 M^{-1} with detection limit of 2 μM. Consequently, probe **5** can be used to estimate a wide range of fluoride ions between 2-644 μM.

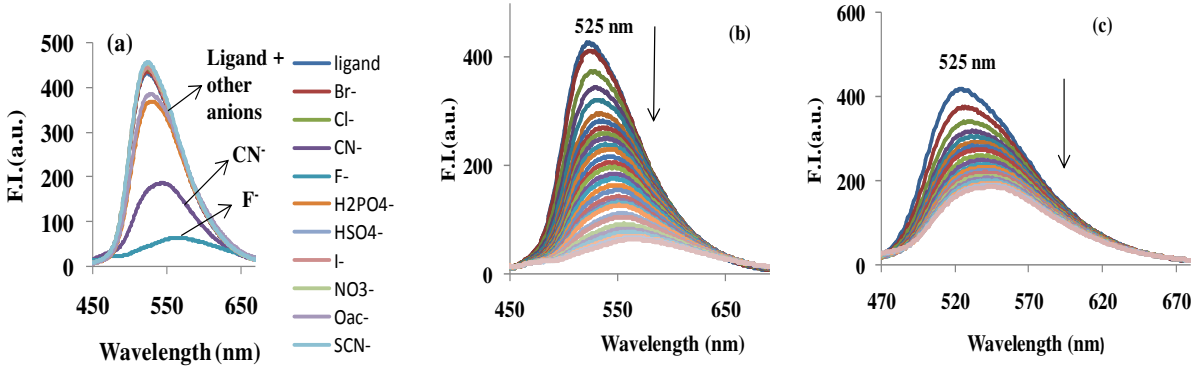

Figure 8: (a) Effect of various anions on emission spectra of probe **5** (20 μM, CH_3CN); (b) Effect of addition of F^- ions on emission spectrum of probe **5** at 20 μM in CH_3CN; (c) Effect of addition of CN^- ions on emission spectrum of probe **5** at 20 μM in CH_3CN.

In case of addition of CN^- ions, quenching of the ligand band and subsequent formation of emission band i.e. at 525 were observed (Figure 8c). The binding constant was calculated to be 1.163 X 10^5 M^{-1} with lowest detection limit of 2 µM. Hence, probe **5** can be utilized to determine a wide range of cyanide ions between the ranges of 2-102 µM.

Practical Applicability of Probe 3 & 5

To determine the practical applicability of probe **3**, competitive anion experiments was carried out in the presence of 10 equivalents of F^- ions mixed with 50 equiv. of each of the other anions such as CN^-, Cl^-, Br^-, AcO^-, I^-, HSO_4^-, NO_3^-, SCN^-, $H_2PO_4^-$. No noteworthy variation in the absorbance intensity was found on comparing the results with the ones in the presence and absence of the other anions (Figure 9a).

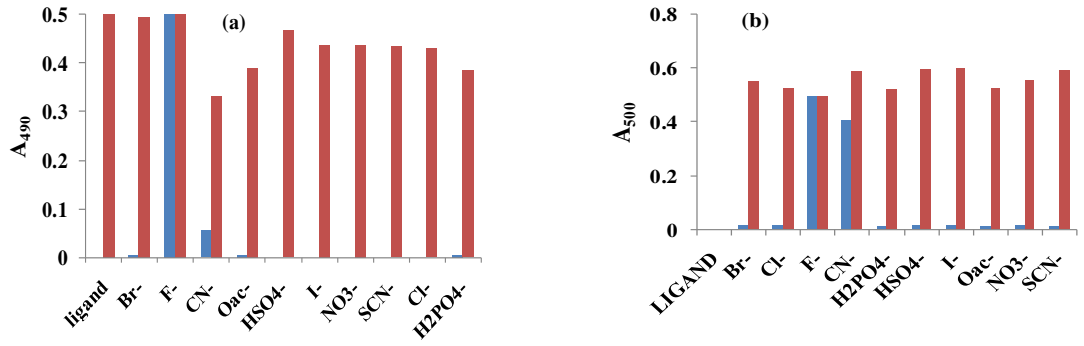

Figure 9: Blue bars represent selectivity of (a) probe **3** (20 µM) (b) probe **5** (20 µM) upon addition of different anions in CH_3CN and red bars shows the competitive selectivity of probe **3** and **5** respectively in the presence of interfering anion.

In order to check the interference of other anions with F^- and CN^- other anions were added (50 equiv. each) such as CN^-, Cl^-, Br^-, AcO^-, I^-, HSO_4^-, NO_3^-, SCN^-, $H_2PO_4^-$ and no significant change in the absorption intensity were observed. To determine the practical applicability of probe **5**, competitive anion experiments was carried out in the presence of 10 equivalents of CN- ions mixed with 50 equiv. of each of the other anions. No noteworthy variation in the absorbance intensity was found on comparing the results with the ones in the presence and absence of the other anions (Figure 9b).

Effect of various metal ions on absorption spectrum of Probe 3 and 5

The chromogenic sensing ability of probe **3** and **5** studied in CH_3CN in the presence of 1000 µM of different cations (Fe^{3+}, Cu^{2+}, Hg^{2+}, Mg^{2+}, Ag^+, Co^{2+}, Pb^{2+}, Zn^{2+}, Ni^{2+}, Ca^{2+}, Al^{3+}, Ba^{2+}

only showed significant color changes in the presence of Fe^{3+} ions respectively (Figure 10 and 11).

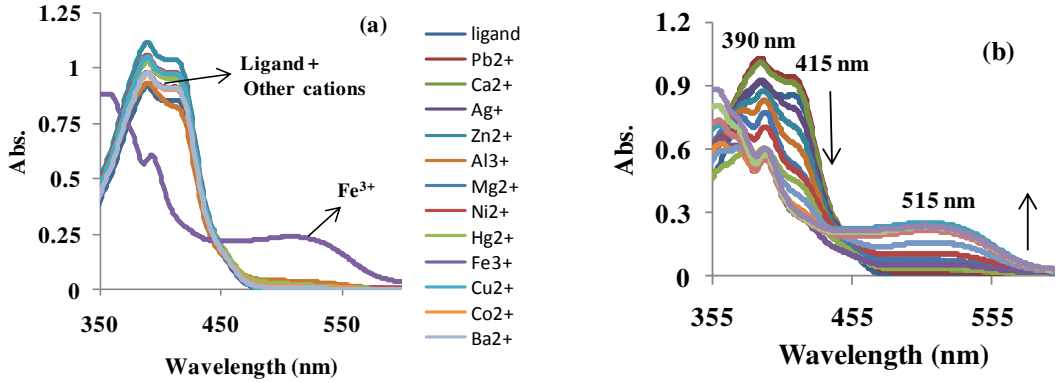

Figure 10: (a) Effect of various cations on absorption spectra of probe **3** (20 μM, CH_3CN); (b) Effect of incremental addition of Fe^{3+} ions on absorption spectrum of probe **3** (20 μM, CH_3CN).

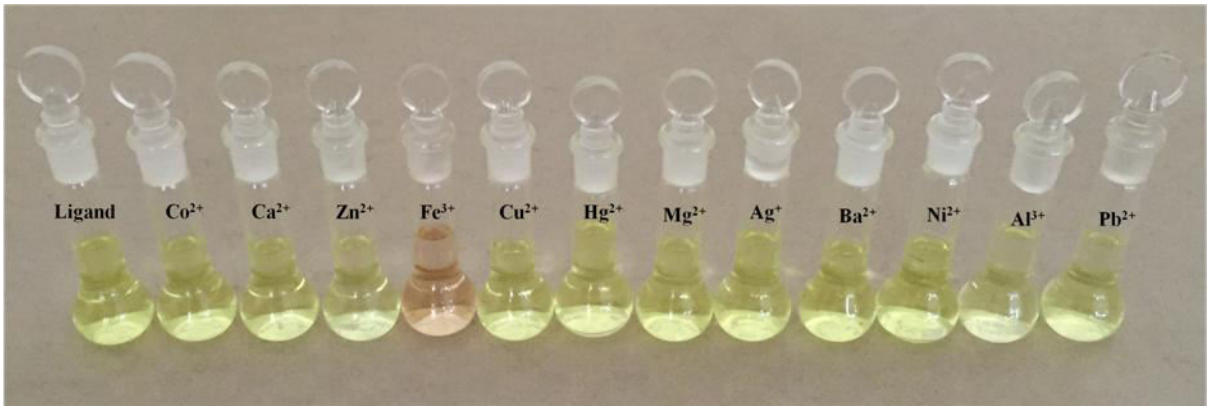

Figure **11**(a): Photographs of probe **3** in the presence of different metal ions at 20 μM in CH_3CN.

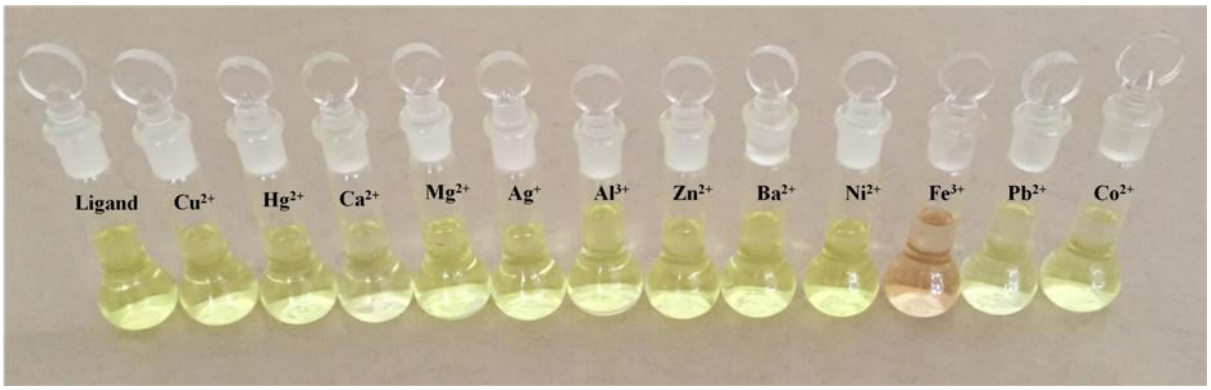

Figure **11**(b): Photographs of probe **5** in the presence of different cations at 20 μM in CH_3CN.

The probe **3** showed the absorption band at 390 nm and 415 nm. Upon addition of Fe^{3+} ions one band was observed in the absorption spectra by 515 nm indicating red shift of 100 nm. Upon gradual addition of Fe^{3+} to the solution of Probe **3** (20 µM in CH_3CN), absorption bands at 390 nm and 415 nm diminished steadily with simultaneous formation of new band at 515 nm with a clear isobestic point at 445 nm till additions up to 100 µM of Fe^{3+} ions, with detection limit of 2 µM (Figure 10b). The Fe^{3+} ion addition resulted in decrease in absorption intensity at 415 nm and increase at 515 nm provided an opportunity to determine Fe^{3+} ions ratio metrically. The absorption ratio varied from 0 to 0.760 at 415 and 515 nm indicating 31.05 fold absorption ratio changes. Thus, probe **3** can be used to estimate an extensive range of Fe^{3+} ions between 2-100 µM through ratio metric approach.

In case of probe **5** the chromogenic sensing ability studied in CH_3CN in the presence of 1000 µM of different cations (Fe^{3+}, Cu^{2+}, Hg^{2+}, Mg^{2+}, Ag^{+}, Co^{2+}, Pb^{2+}, Zn^{2+}, Ni^{2+}, Ca^{2+}, Al^{3+}, Ba^{2+}) only showed significant color changes in the presence of Fe^{3+} ions (Figure 12a). On the other hand, with gradual addition of Fe^{3+} to the solution of Probe **5** (20 µM in CH_3CN), absorption bands at 415 nm diminished steadily with simultaneous formation of new band at 500 nm with a clear isobestic point at 450 nm till additions up to 160 µM of Fe^{3+} ion, with detection limit of 2 µM (Figure 12b). The Fe^{3+} addition resulted in decrease in absorption intensity at 415 nm and increase at 500 nm provided an opportunity to determine Fe^{3+} ion ratio metrically. The absorption ratio varied from -0.0031 to 1.057 at 415 and 500 nm indicating -340.96 fold absorption ratio changes. Thus, probe **5** can be used to estimate an extensive range of Fe^{3+} ion between 2-160 µM through ratio metric approach.

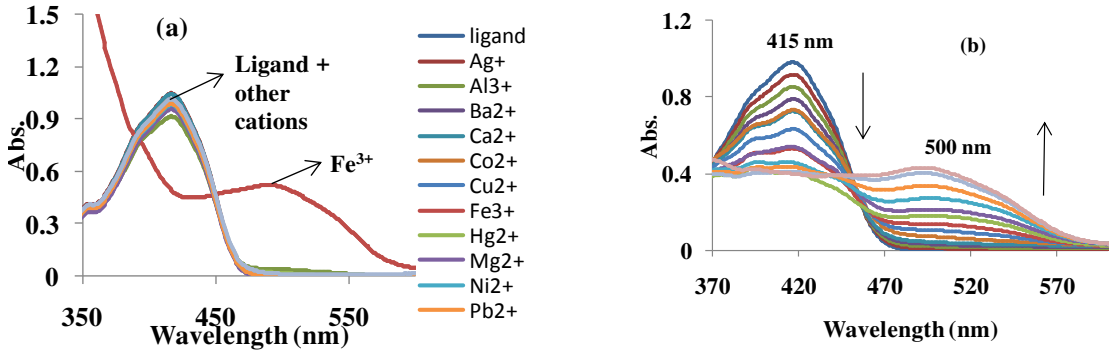

Figure 12: (a) Effect of various cations on absorption spectra of probe **5** (20 µM, CH_3CN); (b) Effect of incremental addition of Fe^{3+} ion on absorption spectrum of probe **5** (20 µM, CH_3CN).

Effect of various cations on emission spectrum of Probe 3 and 5

The probe **3** and probe **5** (20 µM, CH_3CN) on excitation at 390 nm and 420 nm exhibited emission band at 490 nm and 525 nm, respectively. On addition of various cations, no significant change was observed except for Fe^{3+} ion as shown in (Figure 13a and 13b). In case of probe **3,** Enhancement with Fe^{3+} shows the binding effect and in case of probe 5, quenching is observed due to paramagnetic effect of Fe^{3+} which shows there is no binding effect.

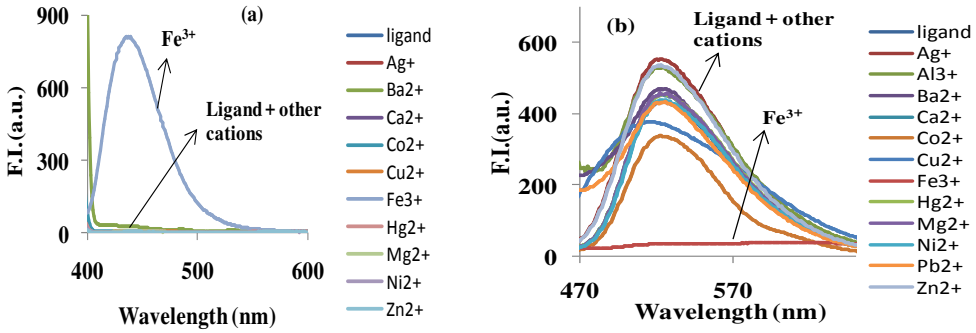

Figure 13: Effect of various cations on emission spectra of probe **3** (20 µM, CH_3CN); (b) Effect of various cations on emission spectra of probe **5** (20 µM, CH_3CN).

In case of probe **3**, the fluorescence enhancement was observed at 490 nm in case of Fe^{3+} ions. To check the binding behaviour of probe **3** towards Fe^{3+} ion, solution of probe **3** was titrated against Fe^{3+} ion. We established that upon addition of 28.75 µM of Fe^{3+} ion, fluorescence intensity was completely enhanced (Figure 14a). The binding constant was calculated to be 7.18 X 10^4 M^{-1} with detection limit of 0.25 µM. Consequently, probe **3** can be used to estimate a wide range of Fe^{3+} ions between 0.25-28.75 µM.

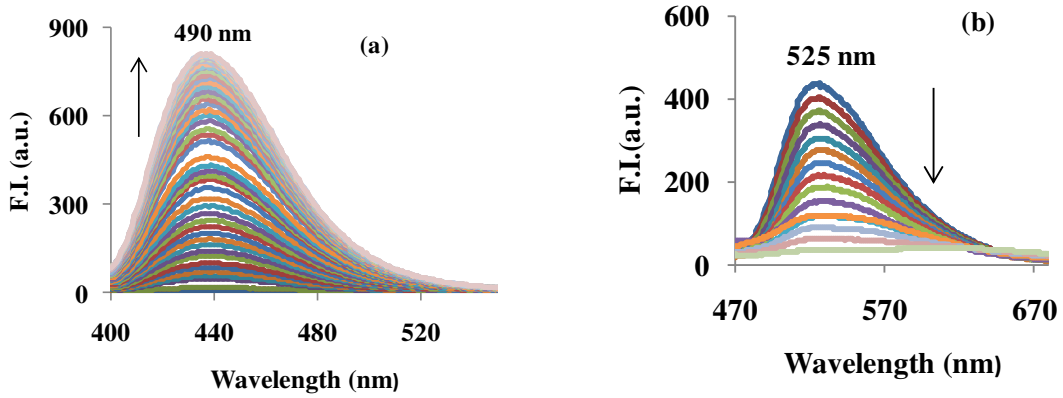

Figure 14: (a) Effect of addition of Fe^{3+} ions on emission spectrum of probe **3** at 5 μM in CH_3CN; (b) Effect of addition of Fe^{3+} ions on emission spectrum of probe **5** at 20 μM in CH_3CN.

In case of probe **5**, the fluorescence quenching was observed at 525 nm in case of Fe^{3+} ions. To check the binding behaviour of probe **5** towards Fe^{3+} ions, solution of probe **5** was titrated against Fe^{3+} ions. We established that upon addition of 200 μM of Fe^{3+} ions, fluorescence intensity was completely quenched (Figure 14b). The binding constant was calculated to be 1.53 X 10^4 M^{-1} with detection limit of 10 μM. Consequently, probe **5** can be used to estimate a wide range of Fe^{3+} ions between 10-200 μM.

Binding behaviour of probe 3 towards Fe^{3+}

To determine complexation behaviour of Fe^{3+} towards probe **3**, Job's Plot was drawn (Figure 15). Stock solution of the same concentration of Probe **3** and Fe^{3+} were prepared of the order of 2.0×10^{-5} (M) in CH_3CN. The absorbance in each case with different host–guest ratio but equal volume was recorded. Job`s plots were drawn by plotting $\Delta I.X_{host}$ vs X_{host} (ΔI = change of intensity of the absorbance spectrum during titration and X_{host} is the mole fraction of the host in each case, respectively) and found that there exists a 1:1 stoichiometry.

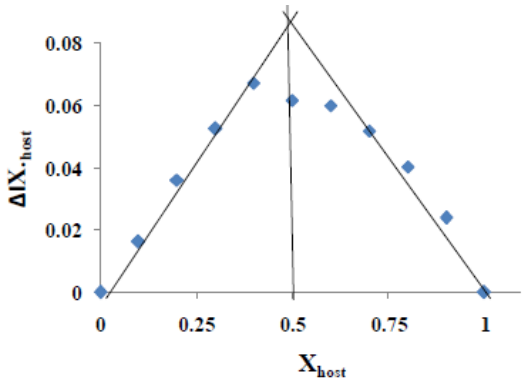

Figure 15: Job's plot diagram of Probe **3** with Fe^{3+} ions in CH_3CN.

Practical Applicability of Probe 3 and Probe 5

In order to check the interference of other cations with Fe^{3+}, other cations were added (50 equiv. each) such as Cu^{2+}, Hg^{2+}, Mg^{2+}, Ag^{+}, Co^{2+}, Pb^{2+}, Zn^{2+}, Ni^{2+}, Ca^{2+} , Al^{3+}, Ba^{2+} and no significant change in the absorption intensity were observed.

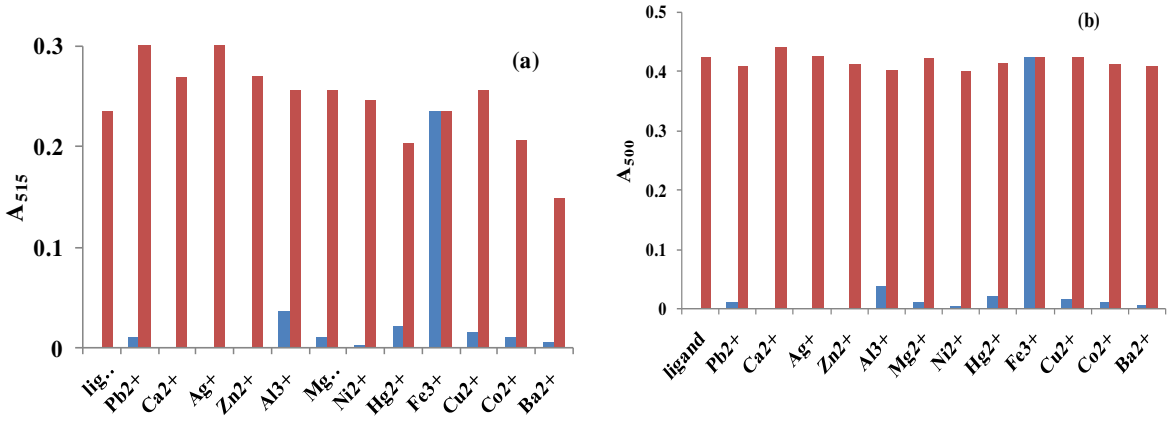

Figure 16: Blue bars represent selectivity of (a) probe **3** (20 μM) (b) probe **5** (20 μM) upon addition of different cations in CH_3CN and red bars shows the competitive selectivity of probe **3** and **5** respectively in the presence of interfering cation

To determine the practical applicability of probe **3** and **5**, competitive cation experiments were carried out in the presence of 10 equivalents of Fe^{3+} ions mixed with 50 equiv. of each of the other cations. No noteworthy variations in the absorbance intensity were found on comparing the results with the ones in the presence and absence of the other cations (Figure 16a and 16b).

EXPERIMENTAL

Materials and equipments

All chemicals were from Spectrochem and Sigma Aldrich Chemical Co and used without further purification. All reactions were monitored by thin layer chromatography. Hexane:Ethyl Acetate was the adopted solvent system. Melting points were recorded by the open capillary tube method and uncorrected. ^{1}H NMR and ^{13}C NMR spectra were carried out using a JEOL ECS-400 MHz spectrometer in SAI Labs, Thapar University, Patiala with TMS as an internal reference. All chemical shifts are reported in ppm relative to the TMS as an internal reference. UV-Vis studies were carried out on a Shimadzu UV-2600 machine using slit width of 1.0 nm and matched quartz cells. Fluorescence spectra were determined on a Varian Cary Eclipse fluorescence spectrometer. Stock solution of probe **3** and **5** was prepared at 10^{-3} M in THF. All absorption and fluorescence scans were saved as ACS II files and further processed in Excel™ to produce all graphs shown. Solutions of **3** and **5** were typically 20 μM for UV-Vis studies. Tetrabutylammonium salt was used for anionic studies and perchlorate salts were used for metal studies. Binding constant was calculated according to the Benesi-Hildebrand equation. K_a was calculated following the equation stated below.

$$\mathbf{1/(A-A_o) = 1/\{K(A_{max}–A_o)\,[M^{x+}]^n\} + 1/[A_{max}-A_o]}$$

Here $\mathbf{A_o}$ is the absorbance of receptor in the absence of guest, A is the absorbance recorded in the presence of added guest**,** $\mathbf{A_{max}}$ is absorbance in presence of added $\mathbf{[M^{x+}]_{max}}$ and **K** is the association constant. To determine the practical applicability of probe **3 a**nd **5**, competitive anion experiments was carried out in the presence of 10 equivalents of F^- ions respectively and CN^- ions mixed with 50 equiv. of each of the other anions. No noteworthy variation in the absorbance intensity was found on comparing the results with the ones in the presence and absence of the other anions. Job plots were drawn by plotting $\Delta I.X_{host}$ *vs* X_{host} (ΔI = change of intensity of the absorbance spectrum during titration and X_{host} is the mole fraction of the host in each case, respectively) and found that there exists a 1:1 stoichiometry.

General procedure for the Synthesis of Probe 3: To a solution of **1**, (0.1 g, 0.73 mmol) and 1-pyrenecarboxaldehyde (0.16 g, 0.69 mmol) in 10 ml dry methanol were added. The reaction mixture was refluxed overnight at 80 °C. After completion of reaction, reaction mixture was allowed to cool to room temperature. The mixture was filtered and washed with

cold methanol, to get the pure probe **3** as yellow colored solid (85 mg, 90% yield), m.p. 240-241^{0}C.

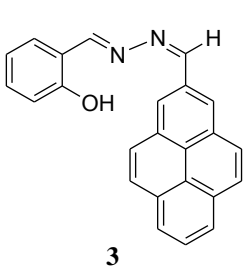

3

^{1}H NMR ($CDCl_3$ + DMSO-d_6, 400 MHz): δ 11.47 (bs, 1H, OH), 9.88 (s, 1H, HC=N), 9.16-9.13 (m, 2H, HC=N and ArH), 8.74-8.72 (d, 1H, *J* = 5.56 Hz, ArH), 8.43-8.25 (m, 6H, ArH), 8.17-8.13 (m, 1H, ArH), 7.74 (d, 1H, *J* = 6.4 Hz, ArH), 7.42 (t, 1H, *J* = 7.32, ArH), 7.02-7.00 (m, 2H, ArH); ^{13}C NMR ($CDCl_3$ + DMSO-d_6, 100 MHz): δ 164.4, 161.7, 159.2, 133.2, 132.8, 132.1, 132.0, 130.8, 130.3, 130.1, 129.2, 129.0, 127.2, 126.5, 126.4, 126.2, 126.0, 125.0, 124.3, 123.8, 123.0, 119.4, 118.0, 116.6 (ArH); ESI 363.12 (M^+1).

General procedure of Synthesis of Probe 5 – To a solution of **4**, (0.1 g, 0.53 mmol) and 1-pyrenecarboxaldehyde (0.12 g, 0.52 mmol) in 10 ml dry methanol were added. The reaction mixture was refluxed overnight. After completion of the reaction, reaction mixture was allowed to cool to room temperature. The mixture was filtered and washed with cold methanol, to get the pure probe **5** as dark yellow colored solid (85 mg, 90 % yield), m.p 247-248 ^{o}C.

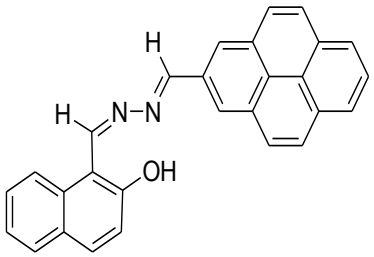

5

^{1}H NMR ($CDCl_3$ + DMSO-d_6, 400 MHz): δ 9.92 (q, 2H, HC=N), 9.14 (d, 1H, *J* = 9.64 Hz, ArH), 8.76 (d, 1H, *J* = 8.24 Hz, ArH), 8.53 (d, 1H, *J* = 8.28 Hz, ArH), 8.46 (d, 1H, J = 8.72 Hz, ArH), 8.40-8.17 (m, 5H, ArH), 8.09 (t, 1H, *J* = 8.0 Hz, ArH), 7.95 (t, 1H, *J* = 8.0, ArH), 7.85 (t, 1H, *J* = 7.4 Hz, ArH), 7.66-7.54 (q, 1H, *J* = 8.72, ArH), 7.41-7.36 (q, 1H, *J* = 6.88, ArH), 7.23 (t, 1H, *J* = 9.16, ArH); ^{13}C NMR ($CDCl_3$ + DMSO-d_6, 100 MHz): δ 161.5, 161.0, 160.6, 160.2, 134.5, 133.2, 131.0, 130.7, 130.2, 129.2, 129.0, 128.8,127.9, 127.3, 126.6, 126.2, 125.0, 123.7, 123.5, 121.3, 120.7, 118.9, 118.7, 108.5, 108.2 (ArH).

Conclusions

- We have synthesized pyrene based Schiff bases to study the photophysical behaviour towards different metals and anions.
- The Schiff bases have been successfully used for the estimation of fluoride and cyanide ions colorimetrically and fluorimetically.
- A selective ratiometric detection of fluoride and Fe^{3+} ions were reached due to its change in binding behaviour.
- An easy and selective method for detection of low concentrations of fluoride and Fe^{3+} ions has been developed.

REFERENCES

1. J. Lehn, *Science,* 1993, **260**, 1762.
2. G. V. Sky, D. N. Reinhoudt and W. Verboom, *Angew. Chem. Int. Ed.,* 2007, **46**, 2366.
3. K. Ariga, J. P. Hill, M. V. Lee, A. Vinu, R. Charvet and S. Acharya, *Sci. Tech. Adv. Mater.,* 2008, **9**, 96.
4. R. Y. Tsien and A. W. Czarnik, *J. Am. Chem. Soc*., 1993, **130,** 1356.
5. A. P. de Silva, H. Q. N. Gunaratne, T. Gunnlaugsson, A. J. M. Huxley, C. P. McCoy, J. T. Rademacher and T. E. Rice, *Chem. Rev*., 1997, **97**, 1515.
6. R. Bissell, A. P. de Silva, H. Q. N. Gunaratne, P. L. M. Lynch, G. E. M Maguire and K. R. A. S. Sandanayake, *Chem. Soc. Rev*. 1992, **21**, 187.
7. I. Stibor and E. V. Anslyn**,** *Top. Curr. Chem.*, 2005, **255**, 163.
8. S. L. Wiskur, H. A. Haddou, J. J. Lavign and E. V. Anslyn, *Acc. Chem. Res*., 2001, **34**, 963.
9. J. Wergedal and D. Baylink, *Science*, 1983, **222**, 330.
10. M. J. Cousins, G. Skowronski and J. L. Plummer, *Anaesth Intensive Care*, 1983, **11**, 292.
11. E. P. Randviir and C. E. Banks, *Trends Anal. Chem*., 2015, **64**, 75.
12. C. J. Frederickson, J. Y. Koh and A. I. Bush, *Nat. Rev. Neurosci*., 2005, **6**, 449.
13. I. H. Scheinberg, A. G. Morell and G. L. Eichhorn, *J. Inorg. Biochem*., **1973**, 306.
14. (a) W. Liu, L. Xu, R. Sheng, P. Wang, H. Li and S. Wu, *Org. Lett*., 2007, **9**, 3829; (b) X. Peng, J. Du, J. Fan, J. Wang, Y. Wu, J. Zhao, S. Sun and T. Xu, *J. Am. Chem. Soc*., 2007, **129**, 1500.
15. (a) F. Oueslati, I.D. Bonnamour and R. Lamartine, *New J. Chem*. 2003, **27**, 644; (b) T. Gunnlaugsson, J. P. Leonard and N.S. Murray, *Org. Lett.* 2004, **6**, 1557; (c) T. Gunnlaugsson, C. T. Lee and R. Parkesh, *Org. Lett.* 2003, **5**, 4065; (d) T. Gunnlaugsson, C. T. Lee and R. Parkesh, *Org. Biomol. Chem*. 2003, **1**, 3265.
16. A. Helal and H. S. Kim, *Tetrahedron*, 2010, **35**, 7097.
17. S. Y. Park and J. E. Kwon, *Adv. Mater.,* 2011, **23**, 3615.
18. N. Chitrapriya, V. Mahalingam, L. C. Channels, M. Zeller, F. R. Fronczek and K. Natarajan*, Inorg. Chim. Acta*, 2008, **361**, 2841.
19. F. Faridbod, M. R. Ganjali, R. Dinarvand, P. Norouzi and S. Riahi, *Sensors*, 2008, **8**, 1645.

20. R. Prabhakaran, R. Huang and K. Natarajan, *Inorg. Chim. Acta*, 2006, **359**, 3359.
21. R. Santillan, A. J. Sanchez, B. Ortiz, V. O. Navarrete and N. Farfanc, *Analyst*, 2015, **140**, 6031.
22. Z. Y. Zhou, S. Q. Jiang, S. P. Zhuo, G. G. Shan, L. B. Xing, H. N. Wang and Z. M. Su, *Dalton Trans*., 2015, **44**, 20830.
23. S. M. Mobin, A. K. Saini, M. Srivastava, V. Sharma and V. Mishra, *Dalton Trans*., 2016, **45**, 3927.
24. F. H. Ko, T. Simon, M. Shellaiah, V. Srinivasadesikan, C. C. Lin, K. W. Sun and M.C. Lin, *New J. Chem*., 2016, **40**, 6101.
25. Y. M. Hijji, B. Bararea, A. P. Kennedya and R. Butcher, *Sens. Actuators*, 2009, **136**, 297.
26. A. T. Wu, W. H. Hsieh, C. F. Wan and D. J. Liao, *Tetrahedron. Lett*., 2012, **53**, 5848.
27. A. T. Wu, Y. J. Chang, S. S. Wu, C. H. Hu, C. Cho and M. X. Kao, *Inorg. Chim. Acta*, 2015, **432**, 25.
28. S. Velmathi and D. Udhayakumari, *Spectrochim. Acta, Part A*, 2014, **122**, 428.
29. N. Guchhait, A. Ganguly, S. Ghosh and S. Kar, *Spectrochim. Acta*, *Part A*, 2015, **143**, 72.
30. Y. Shen, H. Xu, X. Tao, Y. Li and Y. Wei, *Spectrochim. Acta, Part A*, 2012, **91**, 375.
31. N. Guchhait, S. Dalapati, M. A. Alam and S. Jana, *J. Fluorine Chem*., 2011, **132**, 536.
32. M. Rodriguez, G. R. Ortiz, D. P. Domingueza, J. L. Maldonadoa, A. Marco, M. Nava, O. B. Garcia, R. Santillan and N. Farfan, *Sens. Actuators*, 2015, **207**, 511.
33. Z. Y. Yang, L. Fan, J. C. Qin, T. R. Li and B. D. Wang, *J. Lumin*., 2014, **155**, 84.
34. S. Velmathi, D. Udhayakumari, S. Saravanamoorthy and M. Ashok, *Tetrahedron Lett.*, 2011, **52**, 4631.
35. V. K. Gupta, A. K. Singha, M. R. Ganjalic, P. Norouzic, F. Faridbodc and N. Mergua *Sens. Actuators*, 2013, **182**, 642.
36. Y. P. Yen, Y. R. Bhorge, H. T. Tsai, K. F. Huang, A. J. Pape and S. N. Janaki, *Spectrochim. Acta, Part A*, 2014, **130**, 7.
37. D. Chellappa, G. Sivaraman, T. Anand and D. Chellappa, *RSC Advances*, 2012, **2**, 10605.
38. M. Shellaiah, Y. C. Rajan, P. Baluc and A. Murugana, *New J. Chem.*, 2015, **39**, 2523.

39. S. B. Liu, C. F. Bi, Y. H. Fan, Y. Zhao, P. F. Zhang, Q. D. Luo and D. M. Zhang, *Inorg. Chem. Commun.*, 2011, **14**, 1297.
40. H. G. Li, Z. Y. Yang and D. D. Qin, *Inorg. Chem. Comm.*, 2009, **12**, 494.
41. X. H. Jiang, B. D. Wang, Z. Y. Yang, Y. C. Liu, T. R. Li and Z. C. Liu, *Inorg. Chem. Commun.*, 2011, **14**, 1224.
42. C. H. Chen, D. J. Liao, C. F. Wan and A. T. Wu, *Analyst*, 2013, **138**, 2527.
43. S. Sarkar, S. Roy, A. Sikdar, R. N. Saha and S. S. Panja, *Analyst*, 2013, **138**, 7119.
44. A. Sahana, A. Banerjee, S. Das, S. Lohar, D. Karak, B. Sarkar, S. K. Mukhopadhyay and A. K. Mukherjee, D. Das, *Org. Biomol. Chem.*, 2011, **9**, 5523.